J|A|C|S
COMMUNICATIONS

Published on Web 12/21/2005

Facile Synthesis of Tin Oxide Nanoparticles Stabilized by Dendritic Polymers

Venkateswarlu Juttukonda, Robert L. Paddock,† Jeffery E. Raymond, Dan Denomme, Andrew E. Richardson, Laura E. Slusher, and Bradley D. Fahlman*

Department of Chemistry, Central Michigan University, Mount Pleasant, Michigan 48859

Received October 9, 2005; E-mail: fahlm1b@cmich.edu

The size of semiconducting metal oxide nanoparticles has been shown to drastically affect their properties,[1,2] allowing these materials to be used for a range of applications such as gas sensors[3] and catalysis.[4] An intriguing catalytic application of metal oxides is the surface deactivation of organophosphorus-based chemical warfare agents.[5] The increased surface area of nanoparticulate oxides has been reported to increase their activities.[6]

A high band-gap material, such as tin oxide, is especially desirable for gas sensor applications, affording this material a high sensitivity toward reducing gases.[7] There are many routes that have been used for SnO_2 nanoparticle growth, with most reports appearing in the foreign literature and patents. Techniques include thermolysis of organometallic precursors,[8] sol−gel,[9] oxidation of $SnCl_2$,[10] sonochemistry,[11] and hydrothermal synthesis.[12] A few recent reports have utilized surfactants to prevent agglomeration of the nanoparticles.[13] However, none of the microemulsion methodologies have resulted in nanoparticles with diameters <10 nm under ambient reaction conditions.

The architecture of dendritic polymers is well-known to encapsulate a variety of species, such as metals,[14] II−VI semiconductors (e.g., CdS),[15] and organics such as drug molecules.[16] However, the dendritic architecture has not been employed for the controlled growth of semiconducting metal oxide nanoparticles. Herein, we report the synthesis of tin oxide nanoparticles stabilized by a variety of dendritic polymers. In contrast with other reports that utilize high temperatures or moisture-sensitive reagents (e.g., tin chloride), our methodology consists of the simple oxidation of an encapsulated stannate salt via reaction with carbon dioxide under ambient conditions.

For our studies, we employed two fourth-generation dendritic architectures: poly(propyleneimine) (PPI) and poly(amidoamine) (PAMAM), with diaminobutyl cores. For PAMAM, we used both amine- and hydroxy-terminated analogues. As an inexpensive alternative, we also utilized a poly(ethyleneimine) hyperbranched polymer (BASF, FW = 25 000). PAMAM and PPI dendrimers were purchased from Dendritic Nanotechnologies, Inc. and Aldrich, respectively. Deionized ultrafiltered water was obtained from Fisher, and simple vaporization of dry ice was used as the carbon dioxide source for our experiments.

For a typical experiment, an aqueous or ethanolic solution containing sodium stannate and a polymeric host was first stirred for a minimum of 2 h to ensure saturated host−guest chelation. Gaseous carbon dioxide was then bubbled through the room-temperature mixture with vigorous stirring for 30 min, which afforded a light yellow solution. It should be noted that the analogous reaction with sodium aluminate afforded nanoparticles of Al_2O_3 (2−3 nm diameters using TEM analysis), with the stoichiometry confirmed by EDS and elemental analysis.

The best dendrimer:sodium stannate molar ratio was 1:4. If more stannate was introduced, a white cloudy precipitate formed upon reaction with CO_2 due to the presence of free SnO_3^{2-} ions in solution. In addition to affording control over nanoparticle growth, our use of a deficient number of stannate ions results in the majority of primary amines remaining unchelated—available for subsequent reaction/functionalization, if desired. Although we also performed the analogous reactions with CO_2 under supercritical conditions, there were no further benefits from the introduction of high pressure. However, this approach would likely be relevant for higher generation dendrimers or other surface-densified macromolecular hosts.

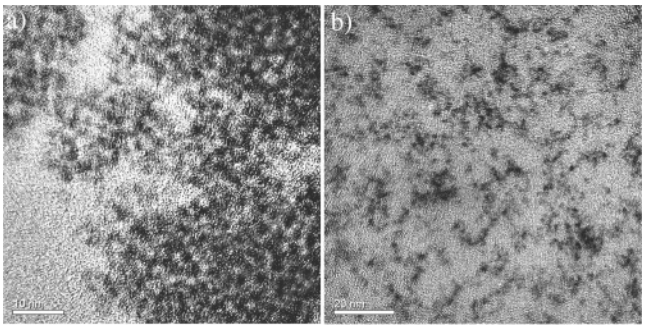

Figure 1. TEM images of SnO_2 nanoparticles immobilized on (a) G4-PAMAM-NH_2 (scale bar = 10 nm) and (b) a poly(ethyleneimine) hyperbranched polymer (scale bar = 20 nm).

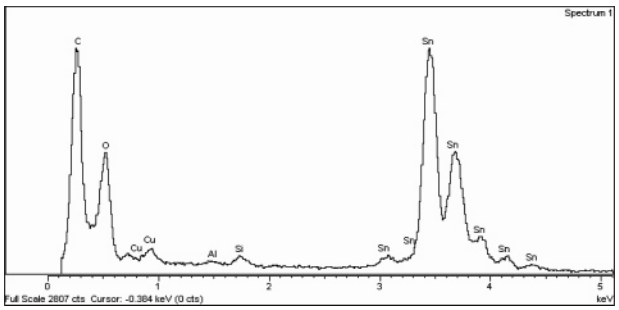

Figure 2. EDS spectrum of the as-grown SnO_2@PAMAM nanoparticles.

Figure 1 shows TEM images of representative SnO_2 nanoparticles. It is unlikely that the dendrimer hosts remain intact in the TEM images due to their thermal sensitivities. For TEM analysis, the suspended nanoparticles were aerosol-sprayed onto carbon-coated Cu grids (Ted Pella). The grids were then dipped into water to remove the adsorbed sodium carbonate byproduct and were air-dried. A representative energy-dispersive X-ray spectrum is shown in Figure 2, illustrating the high purity of the as-grown encapsulated nanoparticles. The 2:1 O:Sn ratio was confirmed by elemental analysis.

Blank experiments were performed in the absence of polymer. In these solutions, a white precipitate formed immediately that was an amorphous agglomeration of bulk SnO_2, as confirmed by SEM/EDS, elemental analysis, and powder XRD.

† Current address: Shell Chemical LP, Houston, Texas 77082.

10.1021/ja056902n CCC: $33.50

Scheme 1. Representation of Our General Methodology for Nanoparticle Growth (shown is a fourth-generation, amine-terminated PPI dendrimer)

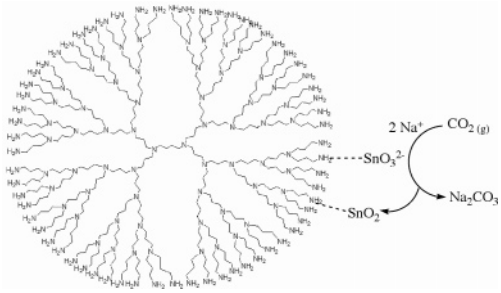

The yield of nanoparticles was greater for amine-terminated PAMAM/PPI dendrimers, relative to hydroxy-terminated analogues that gave rise to significant amounts of large-diameter SnO_2 powder. Using TEM and DLS analyses, the average nanoparticle diameters for $-NH_2$- and $-$OH-terminated PAMAM dendrimers were 3 and 50+ nm, respectively. This is contrary to what is reported for metal encapsulation. For amine-terminated dendrimers, the metal ion is likely chelated to the peripheral groups where final reduction takes place. Usually, the use of surface hydroxyl groups force the ions further within the architecture, resulting in smaller-diameter nanoparticles.[17] However, for our study, the relatively large SnO_3^{2-} ions may be sterically encumbered from entering the interior voids of the dendritic backbone (Scheme 1). The chelation between the Lewis acidic Sn^{4+} site and primary amines is also likely greater than that with interior tertiary amine moieties. In accord with the comparative diameters of PAMAM and PPI dendrimers, we found a slightly smaller diameter for SnO_2 nanoparticles using a PPI host (2.5 nm).

Use of an amine-terminated hyperbranched PEI host also resulted in SnO_2 nanoparticles, with average diameters of 3−3.5 nm. Dynamic light scattering shows a wider diameter distribution relative to PAMAM/PPI, but much narrower than that reported for metal encapsulation using amine-terminated PEI.[18] In general, the lack of extensive agglomeration from $-NH_2$-terminated polymers in our system is likely due to the "buffer" of oxygen atoms that surround the immobilized Sn sites, preventing their cross-linking with neighboring dendrimers.

The experimentally determined hydrodynamic diameter of the G4-PAMAM dendrimer is 4−5 nm.[19] Hence, the larger 6 nm SnO_2 nanoparticle shown in Figure 3 is likely a composite of more than one individual dendrimer unit. This is confirmed by examining the lattice spacings of the nanoparticle, where two separate domains are visible, each with spacings of 3.35 Å, matching the {110} planes of SnO_2.

There are many precedents for the pH-induced variability of metal ion chelation with a dendritic polymer.[20] We performed a similar investigation with the amine-terminated PAMAM dendrimer. It has been shown that for copper encapsulation, as the pH is lowered, the Cu^{2+} ions are moved further within the dendritic architecture rather than bound to the surface primary amines.[14] However, due to the relatively large size of the SnO_3^{2-} ion, a decrease in pH causes the stannate ions to remain unbound, resulting in a white precipitate of bulk SnO_2 upon reaction with CO_2.

In summary, we have successfully synthesized nanoparticles of SnO_2, using a series of dendritic hosts. This work represents the first use of CO_2 as a co-reactant for metal oxide nanoparticulate growth using a dendritic host. Further, we show that controlled growth of small-diameter metal oxide nanoparticles is possible from both structurally precise PAMAM/PPI dendrimers, as well as hyperbranched PEI hosts. The ambient temperature and pressure conditions in our system make this methodology amenable for the synthesis of other metal oxide nanoparticles, for a range of intriguing sensor, nanoelectronic, nanomagnetic, and catalytic applications.

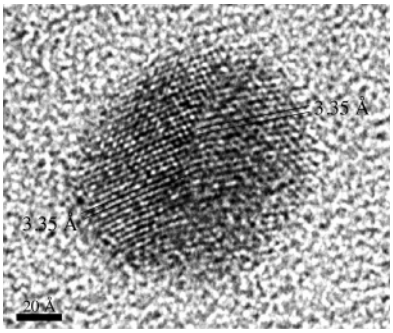

Figure 3. HRTEM image of a SnO_2@PAMAM nanocluster (6 nm diameter), showing the lattice spacings (scale bar = 20 Å).

Acknowledgment. This work is dedicated to the memory of Richard E. Smalley (1943-2005) for his pioneering contributions to nanotechnology. We gratefully acknowledge Dr. Donald Tomalia for his continuing support of dendrimer-related research at CMU. We also thank Drs. Steven McKnight and Lars Piehler at the Army Research Laboratory for funding this and further work. We also acknowledge Research Corporation for a Cottrell College Science Award (CC6045) in support of our ongoing dendritic composite research projects. HRTEM/EDS analysis was performed by Xudong Fan at MSU.

Supporting Information Available: TEM/EDS image of Al_2O_3@PAMAM, and dynamic light scattering (DLS) histograms, showing the polydispersity of all as-grown nanoparticles. This material is available free of charge via the Internet at http://pubs.acs.org.

References

(1) Ramgir, N. S.; Mulla, I. S.; Vijayamohanan, K. P. *J. Phys. Chem. B* **2005**, *109*, 12297.
(2) Diaz, R.; Arbiol, J.; Sanz, F.; Cornet, A.; Morante, J. R. *Chem. Mater.* **2002**, *14*, 3277.
(3) Chaudhary, V. A.; Mulla, I. S.; Vijayamohanan, K.; Hegde, S. G.; Srinivas, D. *J. Phys. Chem. B* **2001**, *105*, 2565.
(4) Harrison, P. G.; Bailey, C.; Bowering, N. *Chem. Mater.* **2003**, *15*, 979.
(5) Ekerdt, J. G.; Klabunde, K. J.; Shapley, J. R.; White, J. M.; Yates, J. T. *J. Phys. Chem.* **1988**, *92*, 6182.
(6) Mitchell, M. B.; Sheinker, V. N.; Cox, W. W.; Gatimu, E. N.; Tesfamichael, A. B. *J. Phys. Chem. B* **2004**, *108*, 1634.
(7) Crooks, R. M.; Zhao, M.; Sun, L.; Chechik, V.; Yeung, L. K. *Acc. Chem. Res.* **2001**, *34*, 181.
(8) Nakamoto, M.; Yamamoto, M. *Kagaku to Kogyo* **2004**, *78*, 503.
(9) Briois, V.; Belin, S.; Chalaca, M. Z.; Santos, R. H. A.; Santilli, C. V.; Pulcinelli, S. H. *Chem. Mater.* **2004**, *16*, 3885.
(10) Jiang, L.; Sun, G.; Zhou, Z.; Sun, S.; Wang, Q.; Yan, S.; Li, H.; Tian, J.; Guo, J.; Zhou, B.; Xin, Q. *J. Phys. Chem. B* **2005**, *109*, 8774.
(11) Zhu, J.; Lu, Z.; Aruna, S. T.; Aurbach, D.; Gedanken, A. *Chem. Mater.* **2000**, *12*, 2557.
(12) Shen, E.; Wang, C.; Wang, E.; Kang, Z.; Gao, L.; Hu, C.; Xu, L. *Mater. Lett.* **2004**, *58*, 3761.
(13) Chen, D.; Gao, L. *J. Colloid Interface Sci.* **2004**, *279*, 137.
(14) For example, see: Balogh, L.; Tomalia, D. A. *J. Am. Chem. Soc.* **1998**, *120*, 7355.
(15) Lemon, B. I.; Crooks, R. M. *J. Am. Chem. Soc.* **2000**, *122*, 12886.
(16) Haag, R. *Angew. Chem., Int. Ed.* **2003**, *43*, 278.
(17) Garcia-Martinez, J. C.; Lezutekong, R.; Crooks, R. M. *J. Am. Chem. Soc.* **2005**, *127*, 5097.
(18) Kramer, M.; Perignon, N.; Haag, R.; Marty, J.-D.; Thomann, R.; Viguerie, N. L.; Mingotaud, C. *Macromolecules* **2005**, *38*, 8308.
(19) Prosa, T. J.; Bauer, B. J.; Amis, E. J.; Tomalia, D. A.; Scherrenberg, R. *J. Polym. Sci., Part B: Polym. Phys.* **1997**, *35*, 2913.
(20) For example, see: Zheng, J.; Stevenson, M. S.; Hikida, R. S.; Van Patten, P. G. *J. Phys. Chem. B* **2002**, *106*, 1252.

JA056902N